Received: 11 May 2023 | Accepted: 19 February 2024

DOI: 10.1111/fcp.13003

ORIGINAL ARTICLE

Fundamental & Clinical Pharmacology | WILEY

Dosing-time, feeding, and sex-dependent variations of everolimus pharmacokinetics in mice

Dilek Ozturk Civelek[1,2] | **Narin Ozturk Seyhan**[2] | **Yasemin Kubra Akyel**[3] | **Isil Gazioglu**[4,5] | **Zeliha Pala Kara**[2] | **Mehmet N. Orman**[6] | **Alper Okyar**[2]

[1]Department of Pharmacology, Faculty of Pharmacy, Bezmialem Vakif University, Istanbul, Turkey

[2]Department of Pharmacology, Faculty of Pharmacy, Istanbul University, Istanbul, Turkey

[3]Department of Medical Pharmacology, School of Medicine, Istanbul Medipol University, Istanbul, Turkey

[4]Department of Analytical Chemistry, Faculty of Pharmacy, Bezmialem Vakif University, Istanbul, Turkey

[5]Applied Analytical Chemistry, Faculty of Chemistry, University of Duisburg-Essen, Essen, Germany

[6]Department of Biostatistics and Medical Informatics, Faculty of Medicine, Ege University, Bornova, Izmir, Turkey

Correspondence
Alper Okyar, Department of Pharmacology, Faculty of Pharmacy, Istanbul University, 34116 Beyazit-Istanbul, Turkey.
Email: aokyar@istanbul.edu.tr

Funding information
This study was financed by the Scientific and Technological Research Council of Turkey-TÜBITAK (project no: 216S475) and the Research Fund of Istanbul University (YOP-24831).

Abstract

Background: Everolimus is an oral mammalian target of rapamycin (mTOR) inhibitor used as an immunosuppressant and anticancer. Its pharmacokinetics is highly variable, it has a narrow therapeutic window and shows chronotoxicity with the best time at ZT13 and worst time at ZT1 (ZT; Zeitgeber time, time after light onset) in the preclinical setting.

Objectives: In the present study, we aimed to investigate whether the pharmacokinetics of everolimus vary according to dosing time and whether sex and feeding status interfere with the chronopharmacokinetics.

Method: A single dosage of 5 mg/kg everolimus was administered orally to C57BL/6J male and female mice, in fed or fasted states at ZT1-rest and ZT13-activity times and blood and tissue samples were collected at 0.5, 1, 2, 4, 12, and 24 h following drug administration. Ileum, liver, plasma, and thymus concentrations of everolimus were determined.

Results: Females had a greater ileum $AUC_{0–24h}$ than males when fed ($P = 0.043$). Everolimus $AUC_{0–24h}$ in the liver was substantially greater at ZT1 than at ZT13 in a fasted state ($P = 0.001$). Plasma C_{max}, $AUC_{0–24h}$, and AUC_{total} were not statistically significant between the groups ($P = 0.098$). In one of the target organs of everolimus, the thymus, males had considerably higher amounts at ZT1 than females ($P = 0.029$).

Conclusion: Our findings imply that the pharmacokinetics of everolimus in mice may differ according to dosing time, sex, and feeding. Greater tissue distribution of everolimus at ZT1 may be associated with the worst tolerated time of everolimus. Our research suggests that oral chronomodulated everolimus therapy may be more effective and safer for cancer patients.

KEYWORDS
chronomodulated chemotherapy, chronopharmacokinetics, everolimus, fed/fasted, sex difference

1 | INTRODUCTION

The circadian timing system (CTS) regulates the majority of mammalian cellular processes and biological functions over a 24-h period, leading to diurnal changes in organism physiology and behavior. The CTS also controls key pathways in the pharmacokinetic and pharmacodynamic processes of anticancer agents. Almost half of the protein-coding genes including proteins

Abbreviations: AKT, protein kinase B; $AUC_{0–24h}$, area under the curve between 0 and 24 h; BCS, Biopharmaceutics Classification System; Cl/F, clearance; Cmax, the maximum concentration; CTS, circadian timing system; CYP, cytochrome; HPLC, high performance liquid chromatography; ICH, International Council on Harmonisation; kel, elimination rate constant; LOD, limit of detection; LOQ, limit of quantification; mTOR, mammalian target of rapamycin; P-gp, P-glycoprotein; PI3K, phosphoinositide 3-kinase; PK, pharmacokinetics; t1/2, elimination half-life; tmax, the time when the maximum concentration is reached; Vd/F, the apparent volume of distribution; ZT, Zeitgeber time.

responsible for drug metabolism and drug transport in mammals display circadian-dependent transcription [1]. Circadian changes in drug pharmacokinetics and pharmacodynamics may cause variations in the efficacy and/or toxicity profiles of drugs. Numerous drugs' pharmacokinetic profiles are time-dependent, and diurnal fluctuations in expressions and activity of metabolic enzymes and drug transporters appear to be the fundamental cause of dosing-time dependence of systemic drug exposure [2–4].

Many published studies show that the pharmacokinetic properties of 5-fluorouracil (5-FU) [5], irinotecan [6,7], cisplatin [8], doxorubicin [9], oxaliplatin [7], tamoxifen [10], erlotinib [11], sunitinib [12,13], seliciclib [14], methotrexate, and orally used capecitabine [15] vary according to the time of application. The delivery of 5-FU, leucoverin, and oxaliplatin in chronomodulated fashion to colorectal cancer patients decreased the dose-limiting adverse effects and toxicity [16]. Strikingly, a meta-analysis by Giachetti et al. revealed that chronomodulated infusion of chemotherapeutics significantly improved therapeutic outcomes in males as compared to flat infusion and the opposite effect was found in females [17]. Innominato et al. also reported that sex influenced the best tolerated time for irinotecan with 5-FU, leucoverin, and oxaliplatin chronomodulated therapy [18]. This observations prove that the sex-related effects should be considered in cancer treatment.

Everolimus is a selective oral mammalian target of rapamycin (mTOR) inhibitor having immunosuppressive and anticancer properties [19]. mTOR is a major serine–threonine kinase in the Phosphoinositide 3-kinase (PI3K)/Protein kinase B (AKT)/mTOR signaling pathway that regulates protein synthesis in relation to cell growth, proliferation, angiogenesis, cell metabolism, and autophagy [20]. It is recognized that this pathway is dysregulated in the vast majority of human malignancies [19,20]. Everolimus is authorized for the treatment of advanced renal cell carcinoma, progressive pancreatic and gastrointestinal neuroendocrine tumors, and breast cancer in postmenopausal women with advanced hormone-receptor-positive, HER2-negative breast cancer in combination with exemestane. Additionally, it is used to prevent organ rejection [21].

According to a recent study, the mTOR signaling pathway is controlled by the circadian clock, and mTOR activity exhibits circadian periodicity. The diurnal variation in mTOR activity has altered the dosing-dependent therapeutic effect of everolimus [22]. Everolimus is predominantly metabolized by cytochrome (CYP) P450 enzymes (CYP3A4, CYP3A5, and CYP2C8) in the liver [21,23]. Everolimus has a large inter-individual pharmacokinetic variability. This variation is attributed to the diverse activities of the drug efflux pump P-glycoprotein (P-gp) and the enzymes CYP3A4, CYP3A5, and CYP2C8 that metabolize everolimus [23]. The dietary pattern also contributes to this inter-individual variability. Food is known to reduce everolimus absorption [24] but it has not been established how this may be affected depending on the dosing time.

In a study conducted by our study group, everolimus was administered to C57BL/6J male mice at different Zeitgeber times (ZT; hours after light onset) ZT1, ZT7, ZT13, and ZT19 for 14 days. Circadian biomarkers, drug-related body weight loss, and clinical observations confirm the best (ZT13) and worst (ZT1) tolerated times. The well-tolerated oral dose of everolimus by the male (5 mg/kg) and female mice (15 mg/kg) was different [25]. Based on this, everolimus was administered to C57BL/6J male (5 mg/kg) and female (15 mg/kg) mice at ZT1 or ZT13 in another setting. Changes in body weight and immunological and hematological toxicity findings showed that the animals experienced higher toxicity at ZT1. These findings were more prominent in the thymus [26]. In pilot research, Giacchetti et al. demonstrated the dose-dependent tolerance of everolimus in patients with metastatic breast cancer. Compared to evening dosing, morning administration of everolimus improved tolerance and adverse effects such as edema, tiredness, and pneumonia [27].

Based on the available information in the literature and our previous preclinical and clinical findings, we aimed to investigate the effects of dosing time (ZT1-rest/worst tolerated time vs. ZT13-activity/best tolerated time), sex, and feeding on everolimus pharmacokinetics. In order to achieve the objective, male and female C57BL/6J mice were administered a 5 mg/kg dose of everolimus orally. This administration was carried out in two distinct states (fed and fasted) and at two distinct times (ZT1-rest and ZT13-activity). The concentrations of everolimus were quantified in plasma, liver, ileum, and thymus at six distinct time points. Better understanding the chronopharmacokinetics of everolimus and adjusting the administration time based on circadian cycles may be a beneficial method for enhancing the therapeutic efficacy of everolimus.

2 | RESULTS

Body temperature rhythms were measured rectally and recorded a day before the experiment. In the dark period body temperatures increased as expected in nocturnally active mice. Diurnal changes in body temperature were found statistically significant ($P < 0.0001$; one-way ANOVA) and rhythmic ($P < 0.0001$; Fourier analysis) both in male and female groups according to ZT (Figure 1).

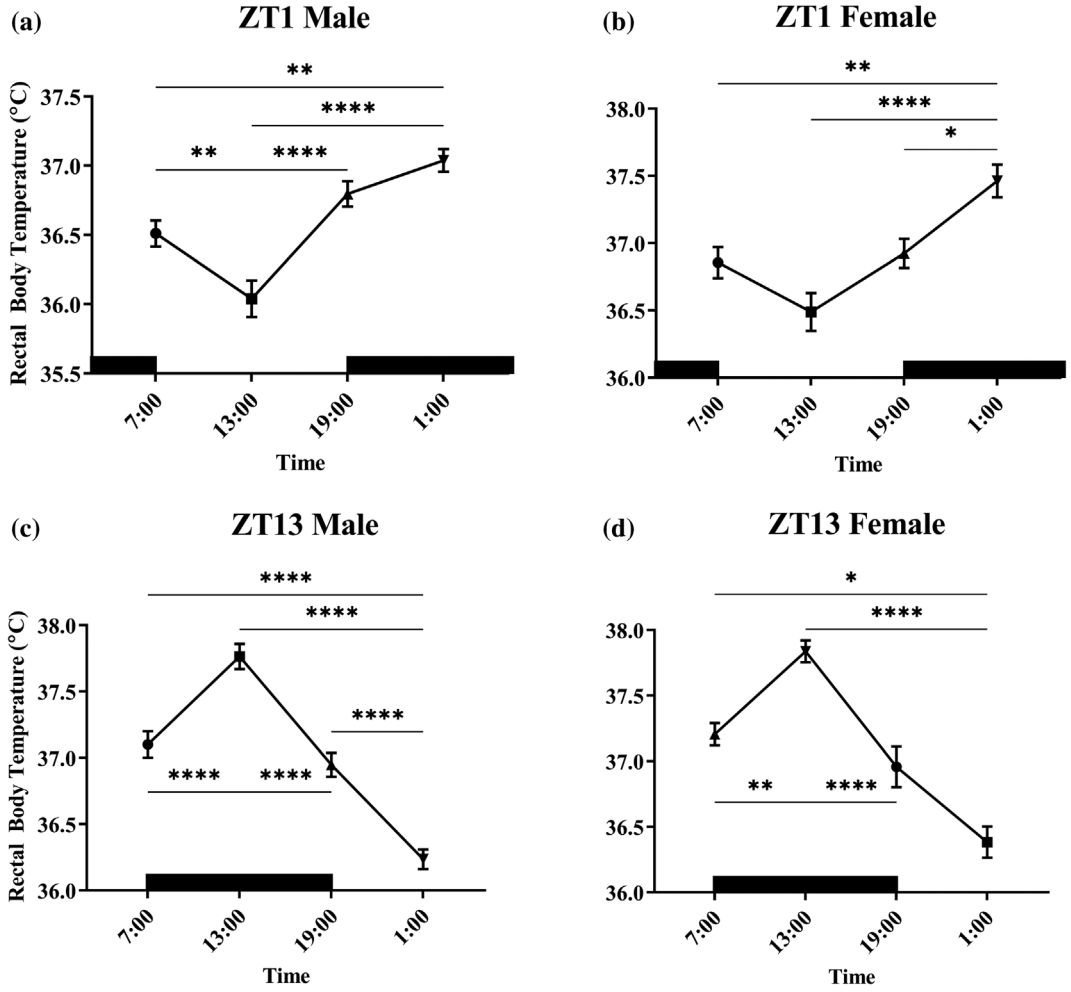

FIGURE 1 Body temperature rhythms measured rectally of ZT1 male (a), ZT1 female (b), ZT13 male (c), and ZT13 female (d) mice. One-way ANOVA; * $P < 0.05$; ** $P < 0.01$; *** $P < 0.001$; ****, $P < 0.0001$.

TABLE 1 Dosing-time dependent pharmacokinetic parameters of everolimus in ileum mucosa in fed or fasted male and female mice.

PK parameters of everolimus	Fed				Fasted			
	Male		Female		Male		Female	
	ZT1	ZT13	ZT1	ZT13	ZT1	ZT13	ZT1	ZT13
t_{max} (h)	1	4	2	1	2	2	1	0.5
C_{max} (μg/g)	3.21 (1.84–3.79)	4.89 (2.26–8.29)	7.91 (4.13–9.83)	12.09 (9.91–12.64)	4.25 (3.42–9.08)	6.98 (0.60–7.54)	3.68 (0.63–13.37)	15.02 (4.60–24.83)
AUC_{0-24h} (μg·h/g)	45.43 (10.73–64.68)	39.93 (17.90–98.17)	105.4 (15.06–119.6)	96.11 (33.59–181.2)	28.15 (17.27–43.71)	43.11 (7.93–222.6)	31.73 (11.95–102.7)	79.72 (17.26–159.7)

Note: The data were presented as median (min – max).
Abbreviations: AUC_{0-24h}, area under the curve between 0 and 24 h; C_{max}, the maximum concentration; PK, pharmacokinetics; $t_{1/2}$, elimination half-life; t_{max}, the time when the maximum concentration is reached.

2.1 | Ileum concentrations and pharmacokinetic parameters of everolimus

All pharmacokinetic parameters of everolimus in ileum tissue are presented in Table 1. Ileum concentration-time graphs are presented in Figure 2 for all groups. C_{max} and AUC_{0-24h} parameters were evaluated according to ZT, feeding status (FS), and sex factors in the ileum. ZT interaction was found statistically different in females, C_{max} values were higher at ZT13 ($P = 0.042$). C_{max} of everolimus affected by sex in the ileum was higher in females at ZT13 ($P = 0.038$) and in fed groups ($P = 0.002$), also higher in females compared to males in the ZT1 fed group ($P = 0.016$). When

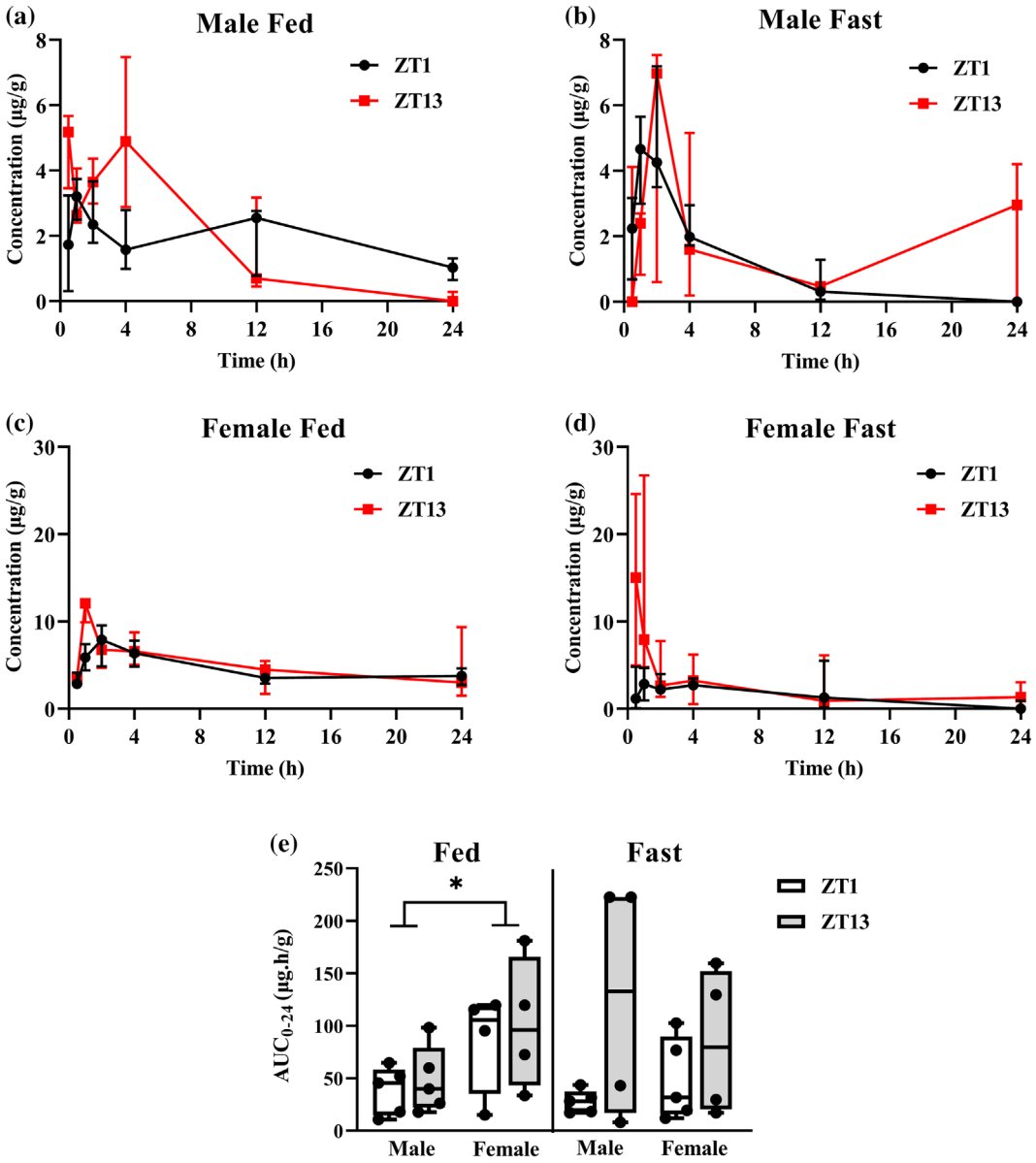

FIGURE 2 Dosing-time dependent concentrations of everolimus in ileum of male fed (a), male fast (b), female fed (c), female fast (d) mice and dosing-time dependent $AUC_{0–24h}$ values of everolimus in ileum of both groups (e). Everolimus ileum concentrations and $AUC_{0–24h}$ values are presented using median (min − max) values according to Zeitgeber time (ZT). In the ileum, the sex*FS interaction for $AUC_{0–24h}$ was statistically significant ($P = 0.08$), but the three-factorial interaction was not ($P = 0.64$). Other statistical comparisons are presented in the text.

$AUC_{0–24}$ of everolimus is investigated only sex and FS are found to affect $AUC_{0–24h}$ values in the ileum. $AUC_{0–24}$ is higher in fed female mice compared to fed males ($P = 0.043$).

2.2 | Liver concentrations and pharmacokinetic parameters of everolimus

The validation results of the method used for the quantification of everolimus from the liver are presented in Table S2. Following oral administration of everolimus, C_{max}, t_{max}, and $AUC_{0–24h}$ in the liver varied according to dosing time, sex, and fasted/fed states (Table 2, Figure 3). C_{max} was affected by FS, it was higher at ZT1 in fasted mice ($P = 0.016$). When $AUC_{0–24h}$ values of the liver are investigated, $AUC_{0–24h}$ was found to be approximately 10-fold higher at ZT1 in fasted mice in both sexes ($P = 0.007$, male; $P = 0.032$, female) (Figure 3e). When we investigated ZT*FS interaction, $AUC_{0–24h}$ was found higher at ZT1 compared to ZT13 ($P = 0.0004$) at fasted state, and fasted $AUC_{0–24h}$ was found higher than fed $AUC_{0–24h}$ at ZT13 ($P = 0.003$). Additionally, when we compared the sex effect on ZT, $AUC_{0–24h}$ was found higher at ZT1 compared to ZT13 in males ($P = 0.0006$) but not in females ($P = 0.068$).

TABLE 2 Dosing-time dependent pharmacokinetic parameters of everolimus in the liver in fed or fasted male and female mice.

PK parameters of everolimus	Fed				Fasted			
	Male		Female		Male		Female	
	ZT1	ZT13	ZT1	ZT13	ZT1	ZT13	ZT1	ZT13
t_{max} (h)	12	0.5	12	0.5	4	0.5	1	0.5
C_{max} (μg/g)	6.54 (2.01–11.18)	3.82 (3.23–9.76)	7.54 (3.71–8.93)	6.52 (4.71–7.80)	16.82 (5.24–28.91)	5.47 (1.07–6.41)	8.79 (8.00–9.12)	4.88 (3.16–9.45)
AUC_{0-24h} (μg·h/g)	116.30 (31.38–184.6)	38.27 (8.06–116.2)	90.09 (26.55–178.0)	77.83 (26.48–123.5)	239.2 (95.62–511.8)	20.32 (0.85–61.29)	66.27 (8.43–140.4)	5.65 (1.71–19.81)

Note: The data were presented as median (min – max).
Abbreviations: AUC_{0-24h}, area under the curve between 0 and 24 h; C_{max}, the maximum concentration; PK, pharmacokinetics; $t_{1/2}$, elimination half-life; t_{max}, the time when the maximum concentration is reached.

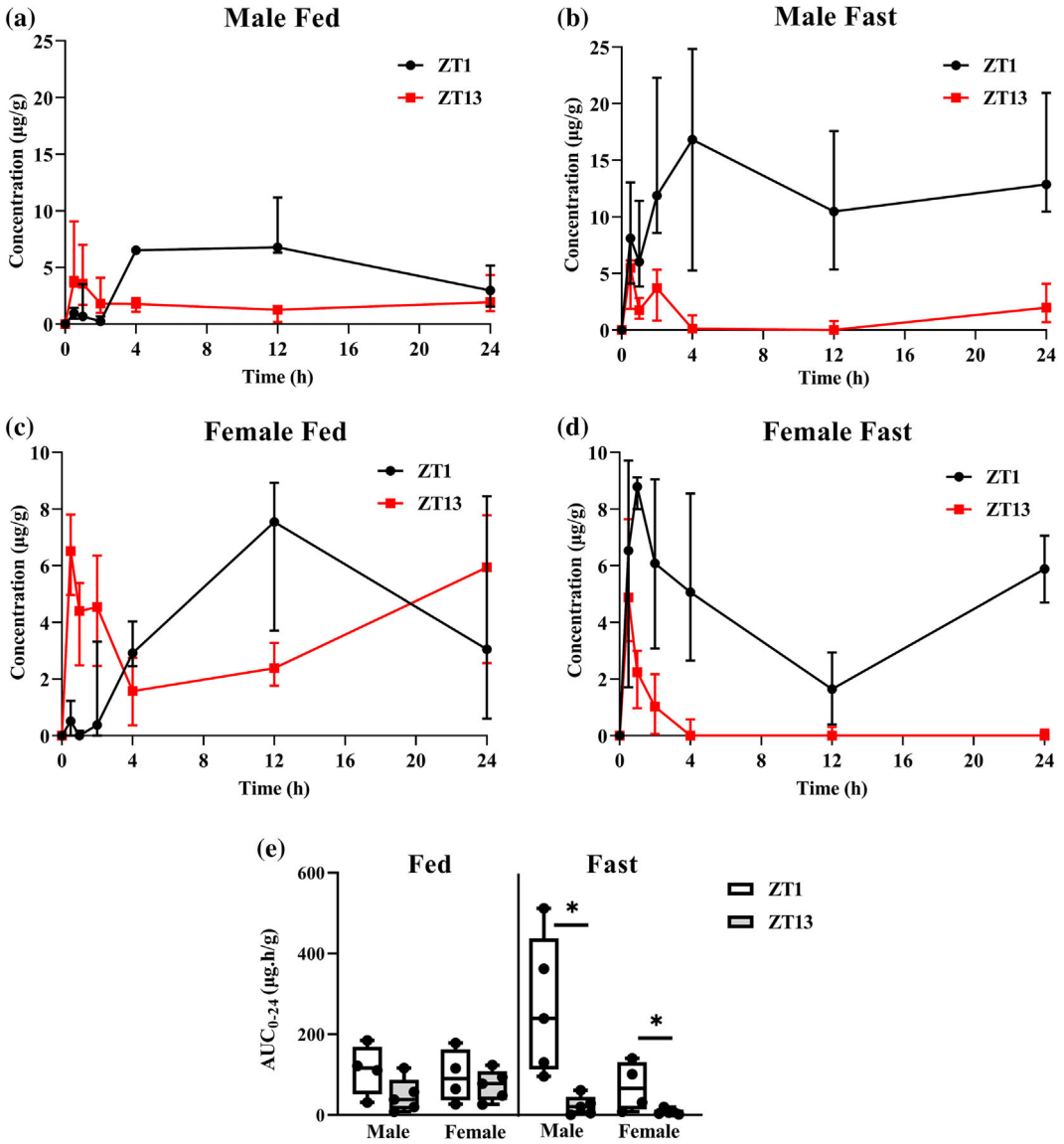

FIGURE 3 Dosing-time dependent concentrations of everolimus in liver of male fed (a), male fast (b), female fed (c), female fast (d) mice and dosing-time dependent AUC_{0-24h} values of everolimus in liver of both groups (e). Everolimus liver concentrations and AUC_{0-24h} values are presented using median (min – max) values according to Zeitgeber time (ZT). In the liver, the ZT*sex interaction for AUC_{0-24h} was statistically significant ($P = 0.046$), but the three-factorial interaction was not ($P = 0.12$). Other statistical comparisons are presented in the text.

2.3 | Plasma concentrations and pharmacokinetics parameters of everolimus

The validation results of the method used for the quantification of everolimus from plasma are presented in Table S1. All pharmacokinetic parameters were evaluated according to ZT, FS, and sex factors in plasma. After oral administration of everolimus, plasma pharmacokinetics varied according to dosing time and sex (Table 3). Plasma concentration-time graphs are presented comparatively in Figure 4 for all groups. Dosing time affected the C_{max} of everolimus in plasma. C_{max} values were higher at ZT13 in both sexes ($P = 0.006$, male; $P = 0.05$, female) and both fed ($P = 0.027$) and fasted ($P = 0.011$) groups, however, only male fed ($P = 0.016$) and female fasted ($P = 0.029$) groups showed statistical dosing time difference when compared individually. Among all groups, the lowest plasma C_{max} value was seen in the ZT1-fed male mice. Plasma everolimus $AUC_{0–24h}$ (Figure 4e) and AUC_{total} were not significantly different according to dosing time ($P = 0.098$). Similarly, related to sex and FS ($P > 0.05$). Plasma clearance (Cl/F, mL/h) was affected by ZT and sex factor when compared individually. Cl/F was higher at ZT1 in males ($P = 0.023$), but not in females ($P = 0.35$). Additionally, it was higher in males than females ($P = 0.029$) at ZT1 and in the fed state ($P = 0.029$). The volume of distribution (Vd/F, mL) was also affected by ZT and sex. Vd/F was higher at ZT1 in males ($P = 0.018$), but not in females ($P = 0.19$), specifically it was higher in fed males compared to females ($P = 0.008$) at ZT1 and compared to ZT13 males ($P = 0.008$). Additionally, Vd/F was higher in males than females at both ZT1 ($P = 0.002$) and ZT13 (0.011) and in both fed ($P = 0.007$) and fasted ($P = 0.0015$) states. FS affected Vd/F in ZT1 male groups, Vd/F was higher in fed state than fasted ($P = 0.016$).

2.4 | Thymus concentrations and pharmacokinetic parameters of everolimus

All pharmacokinetic parameters of everolimus in the thymus are presented in Table 4. There is a dramatic change considering ZT and sex. C_{max} and $AUC_{0–24h}$ values of everolimus in thymus were not significant according to dosing time only ($P > 0.05$) (Figure 5). $AUC_{0–24h}$ was higher in males compared to females at ZT1 ($P = 0.029$). t_{max} varied according to sex, it was higher in males with 24 h compared to females with 0.5–2 h.

3 | DISCUSSION

In this study, we investigated the pharmacokinetics of everolimus depending on the fed-fasted state, sex, and dosing time and aimed to elucidate underlying causes of the chronotoxicity findings of everolimus observed in our previous study which demonstrated that everolimus toxicity was less severe when administered at ZT13 compared to ZT1 [25, 26, 28]. Few research in the scientific literature [27, 29, 30] investigate the pharmacokinetics of everolimus in healthy or tumor-bearing animals. There is only one study that evaluates the pharmacokinetics of intravenously administered everolimus (20 mg/kg, single dose) based on administration

TABLE 3 Dosing-time dependent plasma pharmacokinetic parameters of everolimus in fed or fasted male and female mice.

PK parameters of everolimus	Fed				Fasted			
	Male		Female		Male		Female	
	ZT1	ZT13	ZT1	ZT13	ZT1	ZT13	ZT1	ZT13
t_{max} (h)	2	0.5	0.5	1	0.5	1	2	1
C_{max} (μg/mL)	1.57 (1.44–1.90)	2.70 (2.13–3.28)	2.99 (1.48–3.23)	3.21 (2.80–6.12)	2.39 (1.49–2.94)	2.82 (2.59–3.59)	2.21 (1.97–2.61)	2.66 (2.61–3.67)
$AUC_{0–24h}$ (μg·h/mL)	12.10 (4.83–18.93)	21.77 (5.27–26.57)	21.40 (8.69–29.10)	20.28 (9.25–40.84)	19.06 (12.05–25.49)	22.52 (14.99–30.29)	20.93 (9.07–27.70)	24.81 (13.14–32.88)
AUC_{total} (μg·h/mL)	12.73 (5.10–20.15)	23.28 (6.37–28.09)	22.39 (8.73–30.88)	22.56 (9.31–43.84)	19.38 (12.13–28.97)	23.34 (15.44–38.67)	21.92 (9.30–29.15)	28.01 (14.58–39.05)
$t_{1/2}$ (h)	5.55 (5.02–6.86)	6.03 (4.85–6.19)	5.37 (3.30–6.08)	6.86 (3.10–7.54)	5.68 (3.29–6.08)	4.88 (4.50–10.19)	5.46 (4.28–5.59)	7.07 (3.57–7.54)
Cl/F (mL/h)	8.90 (5.85–12.47)	4.63 (3.08–5.93)	3.98 (2.89–9.85)	4.08 (2.10–5.80)	5.68 (3.86–9.66)	4.71 (2.85–6.79)	4.11 (3.09–8.98)	3.21 (2.30–5.98)
Vd/F (mL)	70.11 (51.81–123.5)	40.96 (21.50–49.72)	30.86 (25.31–46.90)	25.88 (22.83–43.89)	45.77 (33.84–55.15)	41.83 (33.18–44.06)	30.89 (24.90–56.13)	28.59 (25.04–32.79)

Note: The data were presented as median (min − max).
Abbreviations: $AUC_{0–24h}$, area under the curve between 0 and 24 h; AUC_{total}, area under the total curve; Cl/F, clearance; C_{max}, the maximum concentration; PK, pharmacokinetics; $t_{1/2}$, elimination half-life; t_{max}, the time when the maximum concentration is reached; Vd/F, distribution volume.

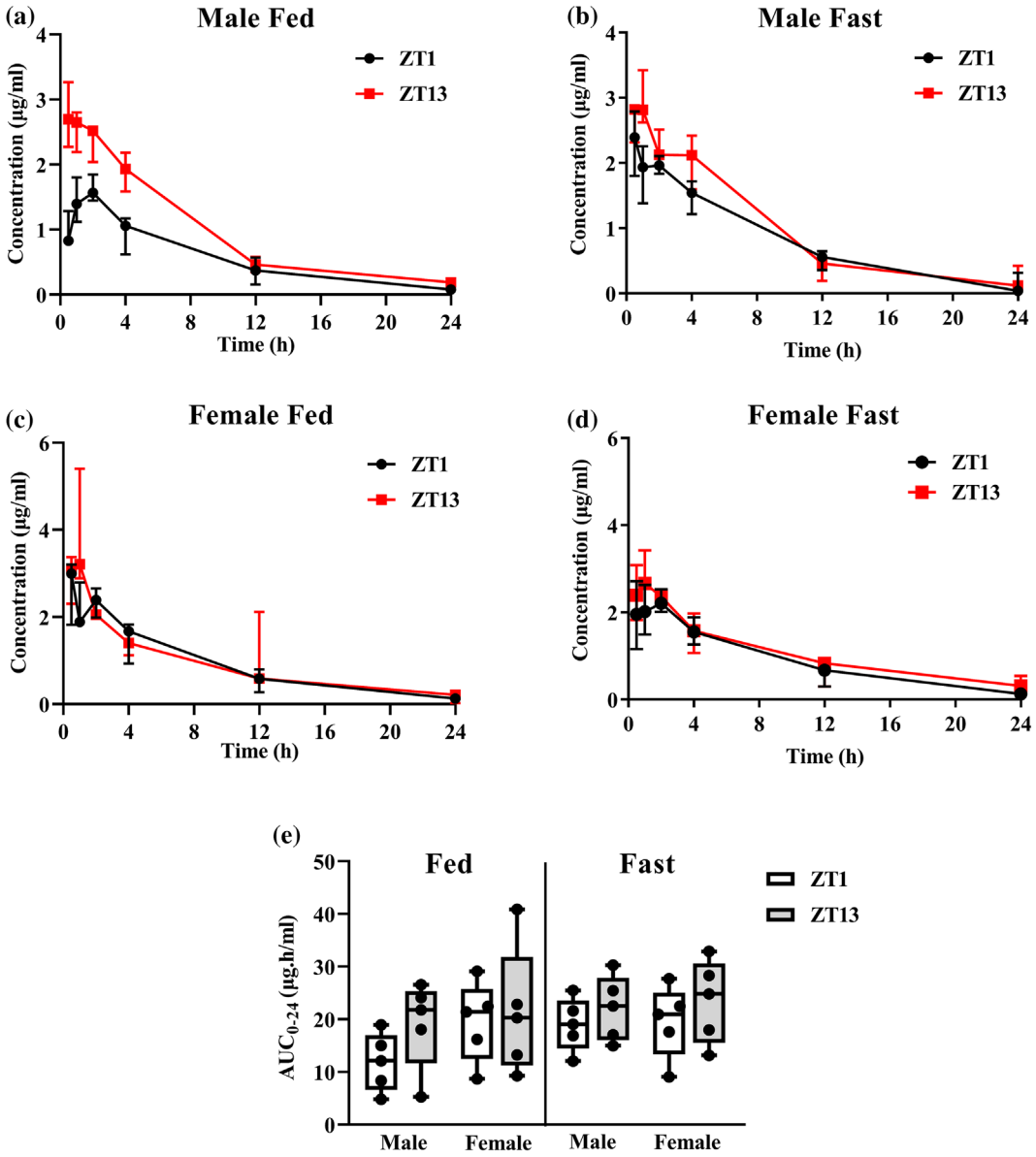

FIGURE 4 Dosing-time dependent concentrations of everolimus in plasma of male fed (a), male fast (b), female fed (c), female fast (d) mice and dosing-time dependent $AUC_{0–24h}$ values of everolimus in plasma of both groups (e). Everolimus liver concentrations and $AUC_{0–24h}$ values are presented using median (min – max) values according to Zeitgeber time (ZT). There was no significance was observed for $AUC_{0–24h}$ in the two or three-factorial interactions in plasma ($P > 0.1$). Other statistical comparisons are presented in the text.

TABLE 4 Dosing-time dependent pharmacokinetic parameters of everolimus in the thymus in male and female mice.

PK parameters of everolimus	Male		Female	
	ZT1	ZT13	ZT1	ZT13
t_{max} (h)	24	24	2	0.5
C_{max} (μg/g)	286.0 (68.61–952.5)	101.2 (7.89–175.7)	41.37 (12.38–177.0)	17.08 (12.99–144.2)
$AUC_{0–24h}$ (μg·h/g)	4388 (1676–7105)	1548 (230.4–2412)	357.1 (29.30–901.7)	247.3 (134.3–401.7)

Note: The data were presented as median (min – max).
Abbreviations: $AUC_{0–24h}$, area under the curve between 0 and 24 h; C_{max}, the maximum concentration; PK, pharmacokinetics; t_{max}, the time when the maximum concentration is reached.

time (ZT0-day and ZT12-night) [22]. Given that everolimus is an orally delivered drug in the clinic and exhibits interindividual differences in its pharmacokinetics, it is reasonable to assess the oral pharmacokinetics of everolimus in terms of dosage time, feeding, and sex-dependence, collectively [23, 31].

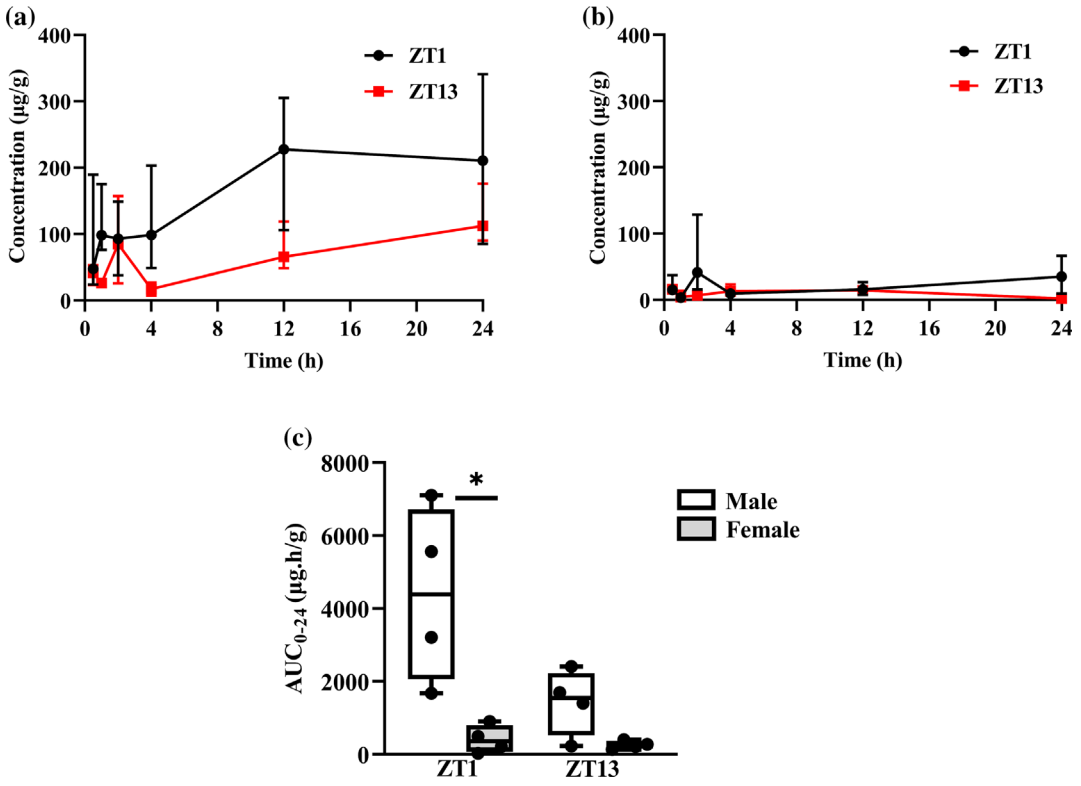

FIGURE 5 Dosing-time dependent concentrations of everolimus in thymus of male (a), female (b) mice and dosing-time dependent AUC_{0-24h} values of everolimus in thymus in both sexes (c). Everolimus thymus concentrations and AUC_{0-24h} values are presented using median (min − max) values according to Zeitgeber time (ZT). The results of the factorial analysis using non-parametric ANOVA showed that no significance was observed in the ZT*sex interaction in thymus ($P > 0.1$). However, sex factor was found significant ($P = 0.002$), but not ZT ($P = 0.125$). Other statistical comparisons are presented in the text.

After oral administration of 5 mg/kg everolimus to mice, dosing time affected C_{max} of everolimus in plasma, which was higher at ZT13 in both sexes and both fed/fasted states ($P < 0.05$). It can be due to greater absorption or rapid elimination of the drug when dosing at ZT13. Plasma clearance (Cl/F, mL/h) was higher at ZT1 in males. Vd/F which indicates the distribution of everolimus was also high in males at ZT1, especially in the fed males. Plasma and liver data were consistent with each other in terms of dosing time-dependent drug exposure. Liver everolimus C_{max} and AUC_{0-24h} values were found to be higher in ZT1 than ZT13 in all groups. The higher distribution of everolimus into the liver at ZT1 can be explained by the slower absorption and slowing down of drug metabolism in the liver during the resting phase (ZT1) [2, 32–34]. Also, the liver/plasma ratio was found to be higher in ZT1, except for ZT1 female groups. This ratio confirms that liver tissue distributions are higher in ZT1. Everolimus is metabolized by CYP3A4 and CYP3A5 [35] and excreted by the multidrug transporter P-gp [60,61] in the liver and intestinal wall. mRNA levels of Cyp3a11 (homologous to human CYP3A4) in the liver of C57BL/6J mice were highest at ZT21 and lowest at ZT1 [36,37]. Mice with lower everolimus detoxification at ZT1 may be the reason for the higher drug accumulation in the liver of ZT1-treated mice. Studies also showed 24-h rhythm in protein and mRNA expression of P-gp in the liver and gastrointestinal tract of mice [37,38]. Okyar et al. demonstrated daily oscillations in P-gp activity in the rats [39] and in mice intestines [40]. In these studies, ileum P-gp activity was higher in the activity phase of mice. Accordingly, the high P-gp expression [40] indicates that everolimus will be excreted more by P-gp into the ileum. This is consistent with our findings, in which everolimus C_{max} and AUC_{0-24h} values in the ileum are higher in fasted mice, especially females, treated at ZT13, but not concordant with fed mice. Although it is known that the drug administration time affects the intestinal absorption of everolimus, it is also influenced by the feeding–fasting status, therefore the systemic exposure of this drug varies depending on the degree of the contribution of these factors.

It is known that the absorption of everolimus decreases with food [24]. Everolimus is a poorly soluble drug in water and has low membrane permeability (Biopharmaceutics Classification System 4; BCS Class IV) [41]. Drugs with these properties may act as Class II (low solubility, high permeability) or Class III (high solubility, low permeability) according to the formulation. Accordingly, when everolimus is taken with

food, C_{max} and $AUC_{0–24h}$ decrease and t_{max} prolongs [24,42]. In the current study, T_{max} was prolonged, and C_{max} and $AUC_{0–24h}$ decreased in male mice in the fed compared to the fasting state.

The effect of food intake on everolimus pharmacokinetics is also observed in ileum data. $AUC_{0–24h}$ decreased in the ileum in all groups in the fasted state compared to the fed groups. The higher presence of everolimus in the ileum of fed mice confirms that the absorption of everolimus decreases with food [24]. In the ileum, C_{max} and $AUC_{0–24h}$ values of everolimus were also dependent on administration time and sex apart from FS, which is very likely due to P-gp expression and activity in mammals. C_{max} of everolimus in the ileum was generally higher at ZT13, and the most prominent ZT1 difference was seen between fasted female groups ($P < 0.05$). The sex-related difference was more pronounced in the fed groups, with $AUC_{0–24h}$ approximately 2-fold higher in females in both ZT ($P < 0.05$). P-gp expression and activity were evaluated by the time of administration, sex, and fasted/fed states using the P-gp substrate talinolol by Okyar et al. [40]. According to Okyar et al., fasting increased the mesor value of P-gp activity and prevented its rhythmicity [40]. This situation contradicts our findings because, in our findings, the everolimus $AUC_{0–24h}$ value in the ileum decreased in the fasted state.

When we investigated ZT*FS interaction in the liver, $AUC_{0–24h}$ was found significantly higher at ZT1 compared to ZT13 at fasted state, and fasted $AUC_{0–24h}$ was higher than fed $AUC_{0–24h}$ at ZT13. When a restriction of food intake is added to the time-dependent effect of drug absorption and metabolism, an increase in liver everolimus distribution may have occurred. Because food intake may reduce the bioavailability of everolimus [24]. Hepatic blood flow is known to increase with nutrients, but its importance in drug absorption and distribution has not been proven [43]. Besides, nutrients may have changed the metabolism of everolimus by influencing Cyp3a4 and P-gp [44–46]. On the other hand, the increase in the bioavailability of everolimus in the fasting state was seen only in ZT1 male mice. This can be explained by the higher drug metabolism at ZT13 (activity phase), and in females than in males [36, 37, 47–49].

Another factor that may affect everolimus pharmacokinetics is sex. Sex changed C_{max} and $AUC_{0–24h}$ of everolimus in the ileum, it was higher in females ($P < 0.05$). The sex-related difference was more pronounced in the fed groups, with $AUC_{0–24h}$ approximately 2-fold higher in females in both ZT ($P < 0.05$). The mesor value of ileum P-gp activity was higher in males than in females. However, P-gp expression in ZT15 was significantly higher in females [40]. Accordingly, the high P-gp expression indicates that everolimus will be excreted more by P-gp into the ileum. This is consistent with our findings, in which the everolimus $AUC_{0–24h}$ value is higher in females in the ileum. The difference between male and female physiology can affect drug pharmacokinetics in various ways. In females, for instance, the gastrointestinal transit time of nutrients is longer, which may increase the absorption of everolimus. However, longer transit time can also increase the interaction time of drugs with intestinal membrane transporters and metabolizing enzymes located in the gastrointestinal mucosa [50]. This may explain the greater amount of unabsorbed everolimus in the ileum of female mice. At the same time, CYP3A4 (homolog to Cyp3a11 in mice) activity, which is responsible for everolimus metabolism, is higher in females [47, 48], which leads to faster metabolism of the drug in the liver and intestine. Although it is known that the hepatic P-gp expression is greater in men than in women, higher expression in females has been observed in mouse studies [40]. This may explain the lower everolimus exposure in female mice in the current study.

Apart from this, the biggest differences between male and female mice were seen in thymus everolimus levels. Everolimus tissue distribution in male mice was substantially greater than in females at ZT1 ($P < 0.05$). This variation in the distribution of everolimus within the thymus was consistent with our prior chronotoxicity investigation in fed male and female mice. In the thymus, both organ weight loss and histopathological results showed higher toxicity at ZT1. Males were more susceptible to everolimus toxicity than females [26]. The toxicity seen in the thymus depending on the dosing time can be explained by the increase in the distribution of everolimus to the tissue in ZT1. Another study by Laplanche et al. showed that the highest binding potential of everolimus was found in the thymus along with the lungs and spleen. Also, tissue affinity was greatest in the thymus along with skin and muscle [51]. Our current chronopharmacokinetics and previous chronotoxicity study [26] showed that tissue affinity and binding potential of everolimus in the thymus may be greater when the drug was administered at ZT1, especially in male mice.

On the other hand, the plasma data of the current study does not explain the cause of the diurnal variation of everolimus toxicity reported in our previous study. In general, the relationship between the blood levels of anticancer drugs and toxicity as a function of time can be established. It is possible to mention such a relationship for methotrexate, an anticancer and immunosuppressant drug [52]. This was not the case for everolimus since higher toxicity was seen in ZT1 which plasma levels are low. However, our liver data indicated that $AUC_{0–24h}$ of everolimus in the liver (i.e., drug exposure) were higher at ZT1 (the most toxic Zeitgeber time for everolimus), and lower at ZT13 (the least toxic Zeitgeber time) in all groups (fed/fasted and male/female), and surprisingly this was particularly more

evident in fasted male mice. We can suggest that plasma levels cannot always reflect the toxicity of a drug, evaluation of the plasma and tissue levels of the drugs together will be a more rational approach, as shown in our study and many others [53, 54]. Similarly, ileum data of the study indicated no significant differences in AUC_{0-24h} values between ZT1 and ZT13, but the difference was more evident according to sex and FS (higher in female and fed mice). The diurnal difference in the ileum, liver, and thymus levels of everolimus appeared to be more evident when given as tissue/plasma ratio (Figures S2–S4), which was higher at ZT1 in each tissue, especially in male mice. These findings are also supportive of our previous study findings of everolimus chronotoxicity [26].

As a conclusion, we indicated that the plasma pharmacokinetics and tissue distribution of everolimus significantly changed according to dosing time, sex, and FS in this study. It is also important in terms of revealing the effect of factors such as feeding (fed/fasted state) and sex (male/female) on everolimus pharmacokinetics. On the other hand, we achieved our goal, albeit partially, with our current study findings, which was to elucidate the underlying causes of everolimus chronotoxicity in mice observed in our previous study. We think that our preclinical study findings will contribute to the attempts to individualize everolimus treatment and optimize the therapeutic outcomes by tailoring chemotherapy to the CTS and sex of the patient. Determining the circadian rhythms in the body and adapting drug therapy to these rhythms, so-called chronotherapy, will improve the tolerability and efficacy of drugs, yet this strategy needs to be further investigated with clinical trials.

4 | MATERIALS AND METHODS

4.1 | Animals and their synchronization

Ten to twelve weeks old C57BL/6J female and male mice (18–25 g) were purchased from Bezmialem Vakif University Experimental Animals Unit, and experiments were performed in the Experimental Animal Care and Accommodation Unit of Istanbul University Faculty of Pharmacy (EDEHAB). The study was conducted according to the ethical guidelines and approved by the Bezmialem University Local Ethics Committee of Animal Experiments (approval no: 2015/253). Mice were housed in polycarbonate cages for up to five animals at standard temperature (22 ± 2°C), illumination (12 h of light/12 h of darkness), and humidity (55 ± 5%). Water and food were given ad libitum. On the experimental days, food restriction was applied only to the animals in the fasting group. Food was discontinued 6 h before drug administration and not given until 4 h later. The procedures to be applied in the dark were performed under dim red light (7×10^4 erg/cm^2). All mice were synchronized for 3 weeks prior to the experiments. Synchronization was controlled by rectal temperature measurement (Testo 108 Thermometer, Harvard App. USA) four times a day (7:00, 13:00, 19:00, and 01:00) for 1 day before the experiment.

4.2 | Experimental study design

The summary of the experimental procedure is visually presented in Figure 6. Everolimus (ApexBio Technology, TX, USA) was freshly prepared by dissolving in propylene glycol:distilled water (50:50, v/v). A single dose of 5 mg/kg everolimus (5 mL/kg) was administered by oral gavage to each experimental animal in both sexes under fasting or ad libitum conditions at different Zeitgeber times (ZT1 and ZT13). Blood and tissue samples were collected at 0.5, 1, 2, 4, 12, and 24 h following drug administration. Five animals were used for a single time point (a total of 240 mice). Blood was taken via cardiac puncture under light isoflurane anesthesia. After exsanguination, the chest was opened, and the left lateral lobe of the liver was removed. Intestines were removed and the ileum was separated. Ileum cleaned with serum physiologic. Then opened longitudinally, the ileum mucosa was scrapped with a clean scalpel tip. The thymus was removed, and all tissue samples were weighted immediately and snap-frozen under liquid nitrogen. All blood samples were collected in EDTA tubes (BD Vacutainer®, NJ, USA), and the tubes were centrifuged at 4000 rpm for 10 min (Hettich, Germany) to obtain plasma. A ratio of 1:1 saline was added to tissue samples, and they were homogenized by a mechanical homogenizer (Art-Miccra-D1, Germany). Plasma and tissue samples were stored at −80°C until the day of analysis.

ZT0 (Zeitgeber Time 0) means light onset, which corresponds to the beginning of the rest phase of the mice. ZT12 is the time of lights off, which corresponds to the beginning of the active phase. Everolimus administration times (ZT1-rest/worst tolerated time vs. ZT13-activity/best tolerated time) were selected according to our preliminary experiments [25].

4.3 | Analysis of plasma and tissue samples

Everolimus in plasma and tissue samples was determined by the validated HPLC-UV method. Everolimus metabolites were not analyzed because they do not contribute to the pharmacological effect. The extraction method was given as supplemental material. Shimadzu HPLC system (Kyoto, Japan) with LC-30AD pump and SPD-20A UV/VIS detector was used for the

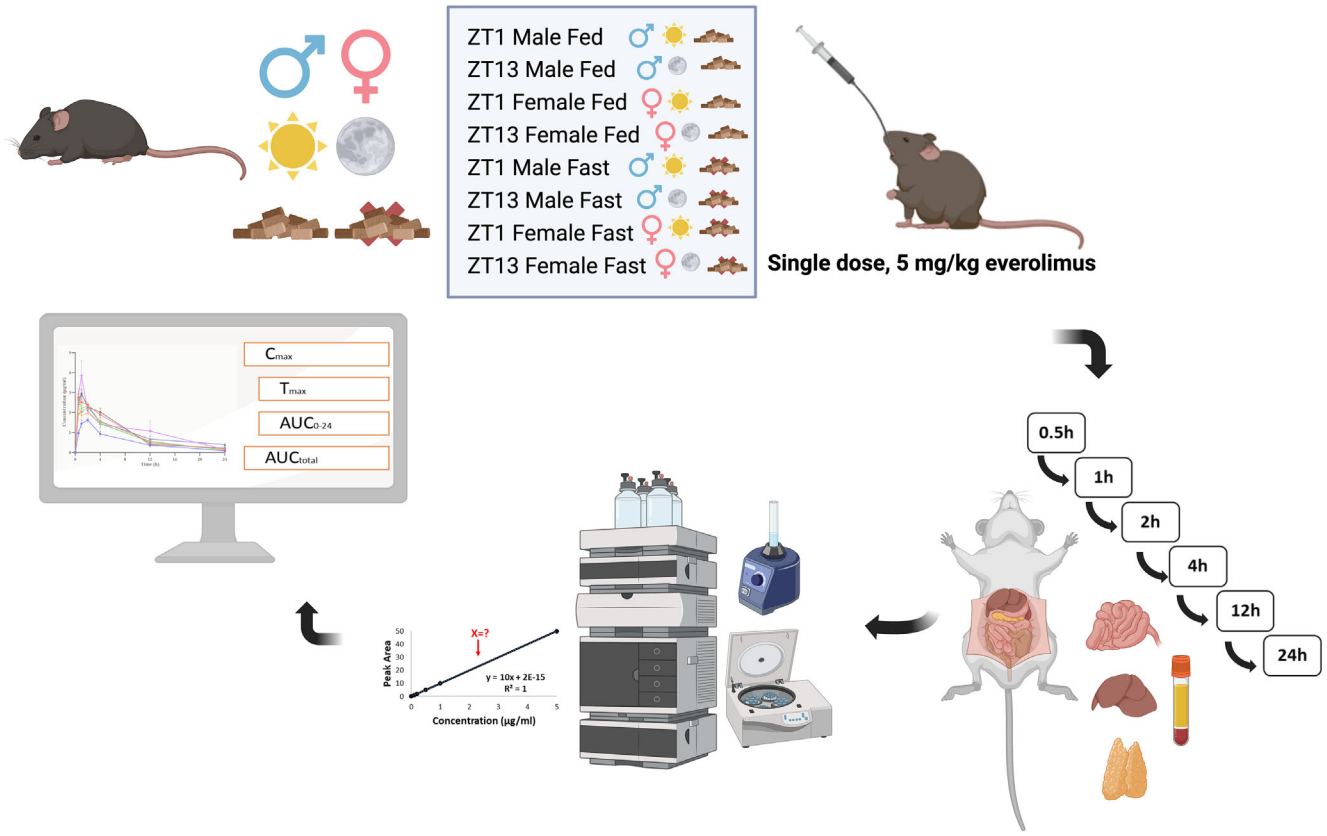

FIGURE 6 The summary of the experimental procedure.

determination of everolimus. Chromatographic separation was carried out on Phenomenex C8 column (100 × 4.6 mm, 5 µm, USA) heated at 50°C and using acetonitrile:ammonium acetate buffer (60:40, v/v, pH 4.0) isocratically at a flow rate of 1 mL/min. Repaglinide (Biocon Limited, India) was used as an internal standard. The chromatographic peaks were detected via a UV detector at 278 nm. Method validation was made according to International Council on Harmonisation (ICH) Guidelines [55]. Linearity, accuracy, sensitivity, specificity, detection limit (LOD), and quantification limit (LOQ) were calculated.

4.4 | Pharmacokinetic calculations and statistical analysis

The pharmacokinetic parameters of everolimus were obtained using the non-compartmental analysis method. Everolimus peak plasma concentrations (C_{max}) and time to reach peak concentration (t_{max}) values were obtained directly from the plasma concentration-time curves of observed experimental data. The area under the plasma concentration-time curve from 0 to 24 h ($AUC_{0–24h}$) was calculated by using the linear trapezoidal rule. The total area under the plasma concentration-time curve from time zero to infinity (AUC_{total}) was calculated as the sum of $AUC_{0–24h}$ and extrapolated part after the last sampling time using the standard formula (concentration at 24 h (C_{24h})/elimination rate constant (k_{el})). k_{el} was obtained by plotting the exponential graph by using the last four time points. Elimination half-life ($t_{1/2}$) was calculated by the equation $0.693/k_{el}$. The apparent total systemic clearance (Cl/F) after the peroral dose was calculated by using the equation $Dose/AUC_{total}$, and the apparent volume of distribution (Vd/F) was calculated by the formula $(Cl/F)/k_{el}$. The pharmacokinetic parameters were presented as median (min – max). A three-way non-parametric ANOVA used to evaluate the effects of ZT, sex, and FS on the $AUC_{0–24h}$. The non-parametric ANOVA was performed via the rankFD package in the R 3.5.2 [56] software using the method (H0F: hypothesis built on distribution functions) developed by Brunner et al. [57–59]. The differences between any two groups were evaluated with Mann–Whitney U test as a subgroup analysis in case of significant interaction. A $P < 0.05$ was considered statistically significant except interaction results (all interaction effects were assessed at 0.1 significance level). Body temperature rhythms were evaluated by spectral analysis through Fourier analysis using IBM SPSS 27.0 (NY, USA). Statistical significance of the sinusoidal 24-h body temperature rhythm was also determined by cosinor analysis. All figures were created with GraphPad Prism version 9.0.0 for Windows, GraphPad Software, San Diego (CA, USA).

AUTHOR CONTRIBUTIONS

Dilek Ozturk Civelek: Conceptualization; investigation; formal analysis; writing—original draft. **Narin Ozturk Seyhan**: Conceptualization; investigation; writing—original draft. **Yasemin Kubra Akyel**: Investigation; writing—review and editing. **Isil Gazioglu**: Investigation; writing—review and editing. **Zeliha Pala Kara**: Funding acquisition; writing—review and editing. **Mehmet N. Orman**: Statistical analysis; review and editing. **Alper Okyar**: Conceptualization; funding acquisition; writing—review and editing.

ACKNOWLEDGMENTS

The authors thank Ferdi Ozturk, Pharm. MSc. for his assistance on the animal studies, Semiha Ozgul, MSc. for her assistance on statistical analysis, and Prof. Durisehvar Unal, Ph.D. for the donation of internal standard repaglinide.

CONFLICT OF INTEREST STATEMENT

The authors are unaware of any relationships, memberships, financing, or financial holdings that could be construed as compromising the objectivity of this work.

ORCID

Dilek Ozturk Civelek https://orcid.org/0000-0003-2485-891X

REFERENCES

1. Takahashi JS. Transcriptional architecture of the mammalian circadian clock. *Nat Rev Genet*. 2017;18(3):164-179. doi:10.1038/nrg.2016.150
2. Lévi F, Okyar A, Dulong S, et al. Circadian timing in cancer treatments. *Ann Rev Pharmacol Toxicol*. 2010;50. Available from: https://pubmed.ncbi.nlm.nih.gov/20055686/
3. Ohdo S. Chronotherapeutic strategy: rhythm monitoring, manipulation and disruption. *Adv Drug Deliv Rev*. 2010;62(9-10):859-875. doi:10.1016/j.addr.2010.01.006
4. Ozturk N, Ozturk D, Kavakli IH, Okyar A. Molecular aspects of circadian pharmacology and relevance for cancer chronotherapy. *IJMS*. 2017;18(10):2168. doi:10.3390/ijms18102168
5. Petit E, Milano G, Lévi F, Thyss A, Bailleul F, Schneider M. Circadian rhythm-varying plasma concentration of 5-fluorouracil during a five-day continuous venous infusion at a constant rate in cancer patients. *Cancer Res*. 1988;48(6):1676-1679.
6. Dulong S, Ballesta A, Okyar A, Lévi F. Identification of circadian determinants of cancer chronotherapy through in vitro chronopharmacology and mathematical modeling. *Mol Cancer Ther*. 2015;14(9):2154-2164. doi:10.1158/1535-7163.MCT-15-0129
7. Lévi F, Karaboué A, Etienne-Grimaldi M-C, et al. Pharmacokinetics of irinotecan, oxaliplatin and 5-fluorouracil during hepatic artery chronomodulated infusion: a translational European OPTILIV study. *Clin Pharmacokinet*. 2017;56(2):165-177. doi:10.1007/s40262-016-0431-2
8. Chen R, Li J, Hu W, Wang ML, Zou SL, Miao LY. Circadian variability of pharmacokinetics of cisplatin in patients with non-small-cell lung carcinoma: analysis with the NONMEM program. *Cancer Chemother Pharmacol*. 2013;72(5):1111-1123. doi:10.1007/s00280-013-2288-5
9. Canal P, Sqall A, de Forni M, et al. Chronopharmacokinetics of doxorubicin in patients with breast cancer. *Eur J Clin Pharmacol*. 1991;40(3):287-291. doi:10.1007/BF00315211
10. Binkhorst L, Kloth JSL, de Wit AS, et al. Circadian variation in tamoxifen pharmacokinetics in mice and breast cancer patients. *Breast Cancer Res Treat*. 2015;152(1):119-128. doi:10.1007/s10549-015-3452-x
11. Liu J, Wang C-Y, Ji S-G, et al. Chronopharmacokinetics of erlotinib and circadian rhythms of related metabolic enzymes in Lewis tumor-bearing mice. *Eur J Drug Metab Pharmacokinet*. 2016;41(5):627-635. doi:10.1007/s13318-015-0284-3
12. Kloth JSL, Binkhorst L, de Wit AS, et al. Relationship between sunitinib pharmacokinetics and administration time: preclinical and clinical evidence. *Clin Pharmacokinet*. 2015;54(8):851-858. doi:10.1007/s40262-015-0239-5
13. Szałek E, Karbownik A, Sobańska K, et al. The influence of the time-of-day administration of the drug on the pharmacokinetics of sunitinib in rabbits. *Eur Rev Med Pharmacol Sci*. 2014;18(16):2393-2399.
14. Sallam H, El-Serafi AT, Filipski E, et al. The effect of circadian rhythm on pharmacokinetics and metabolism of the Cdk inhibitor, roscovitine, in tumor mice model. *Chronobiol Int*. 2015;32(5):608-614. doi:10.3109/07420528.2015.1022782
15. Pilancı KN, Saglam S, Okyar A, et al. Chronomodulated oxaliplatin plus Capecitabine (XELOX) as a first line chemotherapy in metastatic colorectal cancer: a Phase II Brunch regimen study. *Cancer Chemother Pharmacol*. 2016;78(1):143-150. doi:10.1007/s00280-016-3067-x
16. Giacchetti S, Bjarnason G, Garufi C, et al. Phase III trial comparing 4-day chronomodulated therapy versus 2-day conventional delivery of fluorouracil, leucovorin, and oxaliplatin as first-line chemotherapy of metastatic colorectal cancer: the European Organisation for Research and Treatment of Cancer Chronotherapy Group. *J Clin Oncol*. 2006;24(22):3562-3569. doi:10.1200/JCO.2006.06.1440
17. Giacchetti S, Dugué PA, Innominato PF, et al. Sex moderates circadian chemotherapy effects on survival of patients with metastatic colorectal cancer: a meta-analysis. *Ann Oncol*. 2012;23(12):3110-3116. doi:10.1093/annonc/mds148
18. Innominato PF, Ballesta A, Huang Q, et al. Sex-dependent least toxic timing of irinotecan combined with chronomodulated chemotherapy for metastatic colorectal cancer: randomized multicenter EORTC 05011 trial. *Cancer Med*. 2020;9(12):4148-4159. doi:10.1002/cam4.3056
19. Hasskarl J. Everolimus. *Recent Results Cancer Res*. 2018;211:101-123. doi:10.1007/978-3-319-91442-8_8
20. Sánchez-Fructuoso AI. Everolimus: an update on the mechanism of action, pharmacokinetics and recent clinical trials. *Expert Opin Drug Metab Toxicol*. 2008;4(6):807-819. doi:10.1517/17425255.4.6.807
21. Tedesco-Silva H, Saliba F, Barten MJ, et al. An overview of the efficacy and safety of everolimus in adult solid organ transplant recipients. *Transplant Rev*. 2022;36(1):100655. doi:10.1016/j.trre.2021.100655
22. Okazaki H, Matsunaga N, Fujioka T, et al. Circadian regulation of mTOR by the ubiquitin pathway in renal cell carcinoma. *Cancer Res*. 2014;74(2):543-551. doi:10.1158/0008-5472.CAN-12-3241
23. Kirchner GI, Meier-Wiedenbach I, Manns MP. Clinical pharmacokinetics of everolimus. *Clin Pharmacokinet*. 2004;43(2):83-95. doi:10.2165/00003088-200443020-00002
24. Kovarik JM, Hartmann S, Figueiredo J, et al. Effect of food on everolimus absorption: quantification in healthy subjects and a confirmatory screening in patients with renal transplants. *Pharmacotherapy*. 2002;22(2):154-159. doi:10.1592/phco.22.3.154.33542
25. Ozturk N, Okyar A, Li X-M, et al. The circadian timing system as a toxicity target of the anticancer mTOR inhibitor everolimus in mice. *Basic Clin Pharmacol Toxicol*. 2014;318.
26. Ozturk N, Ozturk D, Pala-Kara Z, et al. The immune system as a chronotoxicity target of the anticancer mTOR inhibitor

everolimus. *Chronobiol Int*. 2018;35(5):705-718. doi:10.1080/07420528.2018.1432632
27. O'Reilly T, McSheehy PMJ, Kawai R, et al. Comparative pharmacokinetics of RAD001 (everolimus) in normal and tumor-bearing rodents. *Cancer Chemother Pharmacol*. 2010;65(4):625-639. doi:10.1007/s00280-009-1068-8
28. Ozturk N, Ozturk Civelek D, Sancar S, Kaptan E, Pala Kara Z, Okyar A. Dosing-time dependent testicular toxicity of everolimus in mice. *Eur J Pharm Sci*. 2021;165:105926. doi:10.1016/j.ejps.2021.105926
29. Chu C, Abbara C, Noël-Hudson MS, et al. Disposition of everolimus in mdr1a-/1b- mice and after a pre-treatment of lapatinib in Swiss mice. *Biochem Pharmacol*. 2009;77(10):1629-1634. doi:10.1016/j.bcp.2009.02.013
30. Tang SC, Sparidans RW, Cheung KL, et al. P-glycoprotein, CYP3A, and plasma carboxylesterase determine brain and blood disposition of the mTOR Inhibitor everolimus (Afinitor) in mice. *Clin Cancer Res*. 2014;20(12):3133-3145. doi:10.1158/1078-0432.CCR-13-1759
31. Van Damme-Lombaerts R, Webb N, Hoyer PF, et al. Single-dose pharmacokinetics and tolerability of everolimus in stable pediatric renal transplant patients. *Pediatr Transplant*. 2002;6(2):147-152. doi:10.1034/j.1399-3046.2002.01070.x
32. Musiek ES, Fitzgerald GA. Molecular clocks in pharmacology. *Handb Exp Pharmacol*. 2013;217:243-260. doi:10.1007/978-3-642-25950-0_10
33. Baraldo M. The influence of circadian rhythms on the kinetics of drugs in humans. *Expert Opin Drug Metab Toxicol*. 2008;4(2):175-192. doi:10.1517/17425255.4.2.175
34. Gachon F, Olela FF, Schaad O, Descombes P, Schibler U. The circadian PAR-domain basic leucine zipper transcription factors DBP, TEF, and HLF modulate basal and inducible xenobiotic detoxification. *Cell Metab*. 2006;4(1):25-36. doi:10.1016/j.cmet.2006.04.015
35. Jacobsen W, Serkova N, Hausen B, Morris RE, Benet LZ, Christians U. Comparison of the in vitro metabolism of the macrolide immunosuppressants sirolimus and RAD. *Transplant Proc*. 2001;33(1-2):514-515. doi:10.1016/S0041-1345(00)02116-3
36. Lu Y-F, Jin T, Xu Y, et al. Sex differences in the circadian variation of cytochrome P450 genes and corresponding nuclear receptors in mouse liver. *Chronobiol Int*. 2013;30(9):1135-1143. doi:10.3109/07420528.2013.805762
37. Zhang Y-KJ, Yeager RL, Klaassen CD. Circadian expression profiles of drug-processing genes and transcription factors in mouse liver. *Drug Metab Dispos*. 2009;37(1):106-115. doi:10.1124/dmd.108.024174
38. Ando H, Yanagihara H, Sugimoto K, et al. Daily rhythms of P-glycoprotein expression in mice. *Chronobiol Int*. 2005;22(4):655-665. doi:10.1080/07420520500180231
39. Okyar A, Dressler C, Hanafy A, Baktir G, Lemmer B, Spahn-Langguth H. Circadian variations in exsorptive transport: in situ intestinal perfusion data and in vivo relevance. *Chronobiol Int*. 2012;29(4):443-453. doi:10.3109/07420528.2012.668996
40. Okyar A, Kumar SA, Filipski E, et al. Sex-, feeding-, and circadian time-dependency of P-glycoprotein expression and activity—implications for mechanistic pharmacokinetics modeling. *Sci Rep*. 2019;9(1):10505. doi:10.1038/s41598-019-46977-0
41. Hartinger JM, Ryšánek P, Slanař O, Šíma M. Pharmacokinetic principles of dose adjustment of mTOR inhibitors in solid organ transplanted patients. *J Clin Pharm Ther*. 2022;47(9):1362-1367. doi:10.1111/jcpt.13753
42. Cheung W, Ligia C, Jappe A, Anak O. Pharmacokinetic (PK) profile of a single dose of everolimus (10 mg) administered with a low- or high-fat meal and under fasting conditions in healthy subjects. *JCO*. 2011;29(15_suppl):e15080-e15080. doi:10.1200/jco.2011.29.15_suppl.e15080
43. Tam YK. Individual variation in first-pass metabolism. *Clin Pharmacokinet*. 1993;25(4):300-328. doi:10.2165/00003088-199325040-00005
44. Harris RZ, Jang GR, Tsunoda S. Dietary effects on drug metabolism and transport. *Clin Pharmacokinet*. 2003;42(13):1071-1088. doi:10.2165/00003088-200342130-00001
45. Deferme S, Augustijns P. The effect of food components on the absorption of P-gp substrates: a review. *J Pharm Pharmacol*. 2003;55(2):153-162. doi:10.1211/002235702603
46. Singh BN. Effects of food on clinical pharmacokinetics. *Clin Pharmacokinet*. 1999;37(3):213-255. doi:10.2165/00003088-199937030-00003
47. Hernandez JP, Mota LC, Huang W, Moore DD, Baldwin WS. Sexually dimorphic regulation and induction of P450s by the constitutive androstane receptor (CAR). *Toxicology*. 2009;256(1-2):53-64. doi:10.1016/j.tox.2008.11.002
48. Renaud HJ, Cui JY, Khan M, Klaassen CD. Tissue distribution and gender-divergent expression of 78 cytochrome P450 mRNAs in mice. *Toxicol Sci*. 2011;124(2):261-277. doi:10.1093/toxsci/kfr240
49. Ohno M, Yamaguchi I, Ito T, Saiki K, Yamamoto I, Azuma J. Circadian variation of the urinary 6beta-hydroxycortisol to cortisol ratio that would reflect hepatic CYP3A activity. *Eur J Clin Pharmacol*. 2000;55(11-12):861-865. doi:10.1007/s002280050708
50. Stillhart C, Vučićević K, Augustijns P, et al. Impact of gastrointestinal physiology on drug absorption in special populations—an UNGAP review. *Eur J Pharm Sci*. 2020;147:105280. doi:10.1016/j.ejps.2020.105280
51. Laplanche R, Meno-Tetang GML, Kawai R. Physiologically based pharmacokinetic (PBPK) modeling of everolimus (RAD001) in rats involving non-linear tissue uptake. *J Pharmacokinet Pharmacodyn*. 2007;34(3):373-400. doi:10.1007/s10928-007-9051-7
52. Ohdo S, Inoue K, Yukawa E, Higuchi S, Nakano S, Ogawa N. Chronotoxicity of methotrexate in mice and its relation to circadian rhythm of DNA synthesis and pharmacokinetics. *Jpn J Pharmacol*. 1997;75(3):283-290. doi:10.1254/jjp.75.283
53. Li X-M, Mohammad-Djafari A, Dumitru M, et al. A circadian clock transcription model for the personalization of cancer chronotherapy. *Cancer Res*. 2013;73(24):7176-7188. doi:10.1158/0008-5472.CAN-13-1528
54. Ohdo S, Makinosumi T, Ishizaki T, et al. Cell cycle-dependent chronotoxicity of irinotecan hydrochloride in mice. *J Pharmacol Exp Ther*. 1997;283(3):1383-1388.
55. Singh J. International conference on harmonization of technical requirements for registration of pharmaceuticals for human use. *J Pharmacol Pharmacother*. 2015;6(3):185-187. doi:10.4103/0976-500X.162004
56. Konietschke F, Friedrich S, Brunner E, et al. *Package 'rankFD'*. 2016; (last version June1, 2021). 2016.
57. Brunner E, Bathke AC, Konietschke F. *Rank and pseudo-rank procedures for independent observations in factorial designs: using R and SAS*. 1st ed. Springer International Publishing: Imprint: Springer; 2018last version June; 2018.
58. Brunner E, Konietschke F, Pauly M, Puri ML. Rank-based procedures in factorial designs: hypotheses about non-parametric treatment effects. *J R Stat Soc Series B Stat Methodology*. 2017;79(5):1463-1485. doi:10.1111/rssb.12222
59. Konietschke F, Hothorn LA, Brunner E. Rank-based multiple test procedures and simultaneous confidence intervals. *Electron J Stat*. 2012;6(none):738-759. doi:10.1214/12-EJS691
60. Crowe A, Lemaire M. In vitro and in situ absorption of SDZ-RAD using a Human Intestinal Cell Line (Caco-2) and a single pass perfusion model in rats: comparison with rapamycin. *Pharm Res*. 1998;15(11):1666–1672. doi:10.1023/A:1011940108365

61. Laplante A, Demeule M, Murphy GF, Béliveau R. Interaction of immunosuppressive agents rapamycin and its analogue SDZ-RAD with endothelial P-gp. *Transplant Proc*. 2002;34(8):3393-3395. doi:10.1016/s0041-1345(02)03658-8

SUPPORTING INFORMATION

Additional supporting information can be found online in the Supporting Information section at the end of this article.

How to cite this article: Ozturk Civelek D, Ozturk Seyhan N, Akyel YK, et al. Dosing-time, feeding, and sex-dependent variations of everolimus pharmacokinetics in mice. *Fundam Clin Pharmacol*. 2024;38(5):883-896. doi:10.1111/fcp.13003